Proc. Natl. Acad. Sci. USA
Vol. 96, pp. 9333–9338, August 1999
Medical Sciences

Rifins: A second family of clonally variant proteins expressed on the surface of red cells infected with *Plasmodium falciparum*

SUE A. KYES*†, J. ALEXANDRA ROWE†‡, NELINE KRIEK*, AND CHRIS I. NEWBOLD*§

*Molecular Parasitology Group, Institute of Molecular Medicine, John Radcliffe Hospital, Oxford, OX3 9DS, United Kingdom; and ‡Institute of Cell, Animal and Population Biology, University of Edinburgh, King's Buildings, West Mains Road, Edinburgh, EH9 3JT, United Kingdom

Communicated by David Weatherall, University of Oxford, Oxford, United Kingdom, June 14, 1999 (received for review February 5, 1999)

ABSTRACT **Many pathogens evade the host immune response or adapt to their environment by expressing surface proteins that undergo rapid switching. In the case of *Plasmodium falciparum*, products of a multigene family known as *var* are expressed on the surface of infected red cells, where they undergo clonal antigenic variation and contribute to malaria pathogenesis by mediating adhesion to a variety of host endothelial receptors and to uninfected red blood cells by forming rosettes. Herein we show that a second gene family, *rif*, which is associated with *var* at subtelomeric sites in the genome, encodes clonally variant proteins (rifins) that are expressed on the infected red cell surface. Their high copy number, sequence variability, and red cell surface location indicate an important role for rifins in malaria host–parasite interaction.**

Plasmodium falciparum causes the most severe form of human malaria and is responsible for nearly all malaria-specific mortality. Symptoms occur during the blood stage of infection when parasites undergo cycles of growth and replication within red blood cells. Malaria pathology is linked to parasite-induced changes of the infected red cell surface that mediate adhesion to a variety of host receptors on microvascular endothelium and on uninfected red cells (for review, see ref. 1). This leads to sequestration of infected cells in the microvasculature and rosetting of uninfected red cells, with consequent obstruction to microvascular blood flow (2), tissue damage, and disease (3). The parasite ligands that mediate adhesion to at least some host cell receptors are members of the *P. falciparum* erythrocyte membrane protein 1 (PfEMP1) family (4, 5). These high molecular weight proteins are transported to the surface of the infected red cell, where they have been demonstrated directly to mediate adhesion to endothelial cells via CD36 (6, 7) and to uninfected red cells via complement receptor 1 (8) and heparan sulfates (9). Indirect evidence also suggests that PfEMP1 is the ligand that binds to intercellular adhesion molecule 1 (6, 10). PfEMP1 is therefore considered a major virulence factor, but it also elicits a significant natural antibody response to the parasite that has been implicated in host-protective immunity (11). Reflecting the effects of this immune selection, PfEMP1 undergoes clonal antigenic variation (12, 13) and is encoded by a highly polymorphic multigene family, *var* (13–15). It is the only parasite-derived protein to date that has unequivocally been demonstrated to be exposed on the infected red cell surface by several laboratories (5, 10, 16), but PfEMP1 alone has not been sufficient to explain all parasite-induced surface phenotype changes. Identification of other parasite proteins at the infected red cell surface is, therefore, crucial to our understanding of mechanisms of malaria pathogenesis and immunity.

The publication costs of this article were defrayed in part by page charge payment. This article must therefore be hereby marked "*advertisement*" in accordance with 18 U.S.C. §1734 solely to indicate this fact.

PNAS is available online at www.pnas.org.

While examining early releases of data for chromosome 3 from the *P. falciparum* genome sequencing project, we were struck by a number of features of a second highly polymorphic multigene family known as *rif* (repetitive interspersed family). Although members of this family had been described some years ago and their transcription at late red cell stages had been reported, no protein translation initiation codon could be identified for the available sequences, and protein products were not detected (17). Analysis of the preliminary sequence data suggested that these putative genes coded for membrane proteins of 27–45 kDa and that the initiation codon could be located in a short 5′ exon that resembled a signal sequence. Although the gene family was characterized by relatively conserved 5′ and 3′ ends, the central portion was very highly divergent in different members of the family. The chromosome 2 sequence (18) has also revealed the presence of 17 *rif* genes. Extrapolation to the whole genome from sequence data for both chromosomes suggests that there are in excess of 200 *rif* copies per haploid genome, making them at least four times as abundant as the *var* genes. *Rif* genes are located in close association with *var* genes in clusters within 50 kb of the telomeres, and the name rifins has been proposed for the putative protein products (18) (Fig. 1*a*). Recently, Cheng *et al.* have reported that *rif* genes and the related family known as *stevor* (19) [first reported as *7h8* (21)] are present near the telomeres of all chromosomes (Fig. 1*a*) and have established the intron–exon structure and splice sites for some members. Although *stevor* and *rif* sequences are similar in general size and structure, *stevors* form a distinct, more conserved, lower copy number family.

We were initially prompted to examine *rif* sequences further because their putative membrane protein products were in a similar molecular weight range to the so-called rosettins, reported to be present on the red cell surface and to be involved in the process of rosetting (22). Moreover, their number and high level of sequence diversity was consistent with them being under immune selection and this, combined with their proximity to *var* in the genome, suggested that they might also undergo antigenic variation. In view of these considerations, we undertook to determine the patterns of *rif* gene transcription and the cellular location of the rifin proteins.

MATERIALS AND METHODS

Genome and Sequence Analysis. Sequence data were produced by the *P. falciparum* genome consortium group, for

Abbreviations: PfEMP1, *Plasmodium falciparum* erythrocyte membrane protein-1; RT, reverse transcriptase; RACE, rapid amplification of cDNA ends; GST, glutathione *S*-transferase; IFA, indirect immunofluorescence assay.

Data deposition: The sequences reported in this paper have been deposited in the GenBank database (accession nos. AF161310–AF161312).

†S.A.K. and J.A.R. contributed equally to this work.

§To whom reprint requests should be addressed. E-mail: cnewbold@hammer.imm.ox.ac.uk.

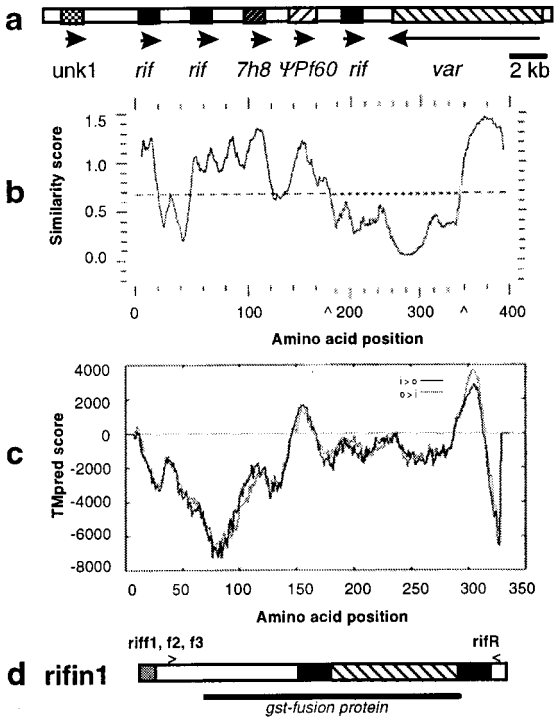

FIG. 1. Genomic organization and sequence analysis of rifins. (*a*) Detail of *P. falciparum* chromosome 3 right subtelomeric region, showing typical orientation of *rif* clusters relative to subtelomeric *var* genes (GenBank accession no. AL010165). The clusters each contain multiple ORFs: several *rif* sequences; *stevor/7h8*, a distinct sequence with some homology to *rif* at the 3′ end (19); novel ORFs (e.g., unk1) of approximately 1 kb; and an apparent pseudogene (ψ) for Pf60 (35), which is highly homologous to the conserved second exon of *var* genes. *Var* is most proximal to the telomere. (*b*) PLOTSIMILARITY profile of 50 rifin sequences. Points above dotted line indicate amino acid positions of high similarity. (*c*) Predicted transmembrane regions and orientation relative to membrane for *rifin1* predicted protein. Positions with positive TMPRED score are possible transmembrane helices; black line indicates scores for pointing outward (i > o), gray line for pointing inward (o > i). Transmembrane regions are amino acids 3–20 (weak, pointing inward), amino acids 145–168 (strong, pointing outward), and amino acids 294–317 (strong, pointing inward). Because of length variation in the highly polymorphic region, the multiple alignment in *b* is longer than the single sequence in *c*. To align *b* with *c*, the *x* axis scale has been reduced in the region between arrows (^). (*d*) Diagram of rifin1 predicted protein, with RT-PCR primer positions indicated (rif f1, f2, and f3 at roughly amino acid position 36–41; rifR at amino acids 318–327). Predicted features of the protein are indicated: signal (shaded), transmembrane regions (solid), semiconserved region and cytoplasmic tail 'inside cell' (open), polymorphic region 'outside cell' (hatched). Relative position of GST fusion protein is indicated by a solid line below.

chromosome 3 at The Sanger Centre (web site http://www.sanger.ac.uk/Projects/P_falciparum/) and for chromosome 2 at The Institute for Genomic Research (http://www.tigr.org). For organization of ORFs at telomere ends, see also ftp://ftp.sanger.ac.uk/pub/databases/P.falciparum_sequences/SUE/IMM-03.gif (right) and ftp://. . ./IMM-04.gif (left). Fifty amino acid sequences used for multiple sequence alignments in Fig. 1*b* are available at site: ftp://ftp.sanger.ac.uk/pub/databases/P.falciparum_sequences/SUE/rif_all. An alignment was performed with the GCG (23) PILEUP program, with default parameters; the resulting alignment file was put through the GCG program PLOTSIMILARITY, giving a plot of the relative amino acid similarities at each position. The positions of putative transmembrane regions of a typical rifin were predicted with programs available at http://www.expasy.ch/tools/, programs TMPRED (24) and TMAP (25, 26). Program SIGNALP (27) was used to determine the likelihood of a cleavable signal sequence at the N terminus of the predicted protein.

Parasites. Parasites were cultured by standard methods and synchronized with sorbitol (28). The PAR^+ parasite clone is as described (22). This parasite has also been named FCR3S1 in some publications (29). The PAR^- parasite line was derived from PAR^+ by selection of nonrosetting parasites by centrifugation of culture suspension through 60% Percoll (Pharmacia). PAR^- is therefore genetically identical to PAR^+ but phenotypically distinct in terms of ability to form rosettes. A4, C10, C18, and R29 are clonal variants derived from the parent clone IT (12). 3D7 and T9/96 are unrelated variants.

RNA Isolation and Northern Blot Analysis. Total RNA was extracted from 0.5 ml of parasitized packed red blood cells at 10% parasitemia by using Trizol reagent (GIBCO/BRL), with the following alterations to the manufacturer's protocol: Trizol reagent was added at 10 times the cell pellet volume for stages up to early pigmented trophozoite and at 20 times pellet volume for later stages (facilitating separation of RNA from DNA); isopropanol precipitation step was extended to at least 2 h at 4°C. RNA was resuspended in formamide; 5 μg was electrophoresed per track on a 2% agarose gel (30) and then capillary-transferred to Hybond-N^+ (Amersham) in 7.5 mM sodium hydroxide. For the complex *rif* PCR fragment probe, three forward and one reverse primer were used. The forward primers were: riff1, CA/GTCACGAG/TTGTTAAGCG; riff2, CGAA/GC/TGTGAATTGTATGC; and riff3, CC/TACC/TAGA/GTTATTATGCG. The reverse primer was rifR, CTTCAA/TATTA/GTTA/TTTTC/TG/TG/A/TCGATAACG. For the complex *var* probe, *varC* primers were used to amplify A4 genomic DNA (31). For PCR, each primer was added at a final concentration of 1 μM, with 20 mM Tris, 50 mM KCl, 2 mM $MgCl_2$, all four dNTPs (each at 200 μM), and 1unit of Perkin–Elmer *Taq* polymerase per 50-μl reaction mixture. Thirty-five cycles were carried out at 94°C for 30 sec, 42°C for 30 sec, and 65°C for 60sec. The resulting PCR product was labeled with [α-^{32}P]dATP (Megaprime kit, Amersham). Blots were hybridized in 7% SDS/0.5 M sodium phosphate/5% dextran sulfate at 50°C and then washed in 0.5× SSC (75 mM sodium chloride/7.5 mM sodium citrate)/0.1% SDS at 55°C.

Pulsed-Field Gel (PFG) Analysis. Chromosomes were separated on pulsed-filed gels (13), and blots were hybridized with the above probes and conditions.

Reverse Transcription (RT)-PCR and Rapid Amplification of cDNA Ends (RACE). For RT-PCR and RACE, PAR^+ and PAR^- RNA samples were treated with DNase I according to the manufacturer's instructions (GIBCO/BRL). For RT-PCR, cDNA was primed by using random hexamers and the first-strand cDNA synthesis kit from GIBCO/BRL; primers and conditions were same as those used for the complex PCR probe (above). RACE was carried out with the 5′ and 3′ RACE kits from GIBCO/BRL, as described by the manufacturer. The following primers were used to amplify the 5′ and 3′ untranslated regions of the *rif* transcript. 5′ RACE reverse primers: gene-specific 1, CATTGTTCTTTACATT; rif1–5R, ACATTGTTTTCGTTTATCTTG; rif3–5R, ACATTTTTGGCGTGTAGTTTTC. 3′ RACE forward primers: rif1–3F, GCTGGTTGTCAAAGGTAAAACTG; rif3–3F, CAGAAAGGAACACTTGAAGCAG.

The primers rifx1F (ATTATTGTCTGCTCTTCCACG) and rif1–5R were used to amplify the genomic region between exon 1 and exon 2. All products were cloned into the TA cloning vector (Invitrogen), then sequenced by using the Perkin–Elmer dRhodamine DNA sequencing kit, and resolved on an Applied Biosystems sequencing system.

Antisera and Western Blot Analysis. Glutathione *S*-transferase (GST) fusion proteins were made by cloning the 5′ conserved domain and central variable region of the *rif1* and

rif3 genes (amino acid 65–292 in rifin1 and amino acids 67–307 in rifin3) into the *Eco*RI and *Xho*I sites of the pGEX-4T-1 vector (Pharmacia). The fragments to be cloned were amplified with the following primers: Rif1F, TCTCGTGAATTCCGTCAAACGTCTGAACGA; Rif1R, GATGCACTCGAGTAAAGCATTAGTAGCAGG; Rif3F, TCTCGTGAATTCCGTCAAACCTCAGAAAGG; Rif3R, GATGCACTCGAGAGTCTGGTAACCTCCATA.

The fusion proteins were expressed in BL21 cells after induction with 1 mM isopropyl β-D-thiogalactoside and were purified on glutathione-Sepharose. Rabbits were immunized as described (32).

For Western blotting, pigmented trophozoites at 8–10% parasitemia were solubilized in Laemelli sample buffer, electrophoresed on a 10% SDS/polyacrylamide gel, and blotted onto nitrocellulose. Immunodetection was carried out with ECL reagents (Amersham) with rifin antisera at a 1:100 dilution and peroxidase-conjugated goat anti-rabbit secondary antibody (Dako) at a 1:2000 dilution.

Immunoprecipitation of Metabolically Labeled and Surface-Labeled Proteins. Late ring/early pigmented trophozoite stage parasites were metabolically labeled by incubating for 4 h with ^{35}S Pro-Mix (Amersham). Cells were solubilized in Triton X-100, and the extracts were immunoprecipitated by using protein A-Sepharose. For surface labeling, iodination of infected cells (20–30% parasitemia) was carried out by using the lactoperoxidase method as described (10). After labeling, cells were treated with trypsin at 1 mg/ml for 5 min, followed by trypsin inhibitor at 2 mg/ml for 5 min. For controls showing effects of trypsin on internal red cell membrane-associated proteins, infected cells were metabolically labeled for 1 h followed by a 4-h incubation in growth medium, then trypsinized, solubilized, and immunoprecipitated. Proteins were electrophoresed on a 10% SDS/PAGE gel (5% for anti-MesA).

Indirect Immunofluorescence Assay. Smears of PAR$^+$ mature pigmented trophozoites were fixed with ice-cold 90% acetone/10% methanol and incubated with a 1:40 dilution of antibody, followed by a 1:50 dilution of FITC-conjugated swine anti-rabbit immunoglobulins (Dako). The parasite nuclei were stained with 4,6-diamidino-2-phenylindole at 1 μg/ml.

Trypsinization, Rosette Formation, and Immunoprecipitation. PAR$^+$ infected red cells were surface-labeled with ^{125}Iodine and then treated with various concentrations of trypsin. Total Triton X-100 soluble extracts and Triton X-100 soluble extracts immunoprecipitated with *rif3* antiserum were electrophoresed on 15% SDS/polyacrylamide gels. After trypsinization, the infected cells were resuspended in malaria culture medium (with 10% heat-inactivated human serum) and assessed for rosetting by microscopy as described (8).

RESULTS

Rifin Structure Predictions. The general structures of both *rif* and *stevor* genes and their predicted protein products have been described (18, 19). Herein we only consider the data on *rif*. Multiple sequence alignments of 50 predicted rifin amino acid sequences show relative positions of semiconserved and polymorphic regions (Fig. 1*b*). The N-terminal half of the sequence contains multiple short polymorphic and semiconserved regions and is cysteine-rich. The C-terminal half of the sequence is highly polymorphic, ending in a short semiconserved region. Program TMPRED (Fig. 1*c*) and the multiple sequence alignment based program TMAP (data not shown) predict two transmembrane regions, at amino acids 145–168 and amino acids 294–317 for rifin1 and in similar positions in the other rifin sequences used in the multiple sequence alignment. Most, but not all other transmembrane prediction programs available at the ExPASy tools web site support this prediction. The N terminus suggests that it is a weak transmembrane candidate, possibly a cleaved signal peptide [program SIGNALP (27)]. Comparing the positions of conserved and polymorphic regions to the predicted transmembrane plot (Fig. 1 *b* and *c*), the transmembrane regions are semiconserved, and the protein has a suggested orientation with the relatively conserved N-terminal half and the semiconserved C terminus (amino acids 318–337) inside the cell, and the highly polymorphic region (amino acids 169–293) outside the cell (Fig. 1*d*). This preferred predicted structure, with the most polymorphic region exposed on the cell surface, would clearly be consistent with immune or functional selection.

Transcription of *rif* Genes. To investigate the transcription of *rif* genes in asexual stage parasites, we used a complex *rif* probe in Northern blot analysis. The probe was made by amplifying genomic DNA from the rosetting parasite clone Palo Alto (PAR$^+$) with oligonucleotide primers designed to amplify multiple *rif* genes (relative primer positions indicated in Fig. 1*d*). The design of truly universal *rif* primers proved to be difficult due to the high degree of diversity between *rif* sequences (see *Discussion*). To determine the utility of the resulting PCR products as a probe, we labeled this complex mixture and hybridized it at high stringency to PAR$^+$ chromosomes separated by pulsed-field gel electrophoresis (data not shown). All chromosomes except the smallest hybridized, showing that this PCR product did indeed contain sequences from many different *rif* loci. The same labeled products were then used to probe Northern blots of RNA taken at various time points from the nonrosetting PAR$^-$ line. At high stringency, bands of approximately 1.8 and 2.1kb were present in a restricted time window, with maximum expression at the late ring/early pigmented trophozoite stage (18–23 h after red cell invasion; Fig. 2*a*). For comparison, the same Northern blots in Fig. 2 were probed with the generic *varC* (*var* exon 2) probe (data not shown). *Var* genes are transcribed as early as 5 h after invasion and increase expression through the late ring stage but decrease significantly in early pigmented trophozoite stages, just as *rif* genes are reaching maximum transcription. The same temporal pattern of *var* and *rif* gene expression was seen with the unrelated parasite clone A4 (data not shown).

***Rif* Transcription Varies Between Isolates.** Having established the life-cycle stage at which *rif* transcription was maximal, we then went on to examine *rif* transcription in a series of parasite clones. For these experiments we used both genetically unrelated parasites (PAR, T9/96, and 3D7) and members of a clone tree which were all originally derived from a single organism of the IT lineage (A4, C10, and C18), as well as the rosetting clone R29, which was also derived at an earlier stage from IT. When the *rif* complex probe was hybridized to Northern blots of RNA prepared from the appropriate stages, it was clear that *rif* expression differs between clones (Fig. 2*b*). The *rif* RNA doublet was detected in PAR$^+$ and PAR$^-$ and in parasite clones A4, C10, and C18. No *rif* transcription could be detected in R29, nor was it expressed in parasites T9/96 or

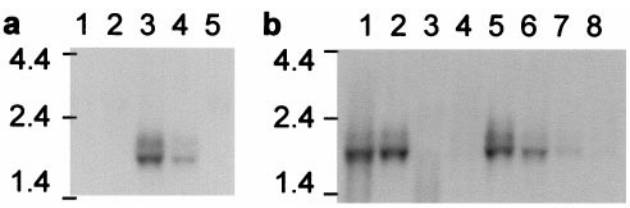

FIG. 2. Transcription of *rif* genes. Northern blot analyses of RNA, hybridized with a complex PAR$^+$ *rif* probe. RNA standards are in kb. (*a*) Stages of PAR$^-$ parasite RNA in the erythrocytic life cycle. Lanes: 1, early rings (0–5 h after invasion); 2, middle rings (8–13 h); 3, late rings/early pigmented trophozoites (18–23 h); 4, early/mature pigmented trophozoites (24–29 h); 5, schizonts (42–47 h). (*b*) RNA from various parasites (late ring/early pigmented trophozoite stage): Lanes: 1, PAR$^+$; 2, PAR$^-$; 3, T9/96; 4, R29; 5, A4; 6, C10; 7, C18; 8, 3D7.

3D7. The same *rif* probe hybridized to all 14 chromosomes of parasites other than Palo Alto in pulsed-field gel chromosome separation blots, showing that the probe was capable of detecting a wide range of *rif* sequences in many isolates.

Expressed *rif* Sequences in Palo Alto Parasites. To determine which members of the *rif* family were transcribed in Palo Alto parasites, we carried out RT-PCR on PAR^+ and PAR^- RNA with the above primers and conditions and cloned the resulting 900-bp PCR products (data not shown). Six clones from each parasite were sequenced. In PAR^+ each sequence was identical (termed *rif1*, GenBank accession no. AF161310). In PAR^-, four of six clones were identical to *rif1* and the other two clones were distinct (*rif2*, accession no. AF161312 and *rif3*, accession no. AF161311). Comparison of the sequences revealed that they were clearly members of the *rif* family but had no other obvious relationship to each other. We confirmed the splicing of the main ORFs of *rif1* and *rif3* to short putative signal peptides by extending these sequences in 5′ and 3′ directions with RACE.

Protein Products of *rif* Genes and Their Cellular Location. Using the sequences obtained above, we expressed *rif1* and *rif3* as GST fusion proteins (relative position indicated in Fig. 1*d*) and used the purified protein to immunize rabbits. The resulting antisera, after exhaustive absorption with uninfected red cells, were used to probe Western blots of Palo Alto asexual blood stage proteins separated by SDS/PAGE. Both antisera recognized proteins of 35 kDa, 36 kDa, 39 kDa (faint), and 44 kDa in PAR^+ and 36 kDa, 39 kDa (faint), and 44 kDa in PAR^- (Fig. 3*a*, lanes 2 and 3. Data for *rif1* antibody not shown). The 30-kDa band present in all tracks was nonspecific, because it was also detected by preimmune rabbit serum (data not shown). The *rif* antisera were next used to immunoprecipitate proteins from metabolically labeled extracts of PAR^+ parasites. Proteins of 35, 36, 39, and 44 kDa were detected, confirming that the proteins of these molecular masses were parasite-derived (Fig. 3*b*, lane 2). The antisera therefore recognize proteins within the predicted size range (35–44 kDa), by immunoprecipitation and by Western blotting. *Rif* genes are thus transcribed and translated into rifins in asexual blood stage parasites.

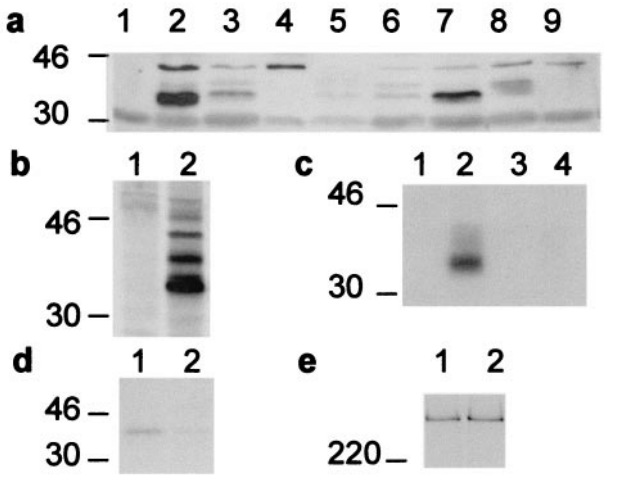

FIG. 3. Expression of rifin proteins. (*a*) Western blot analysis of extracts from various parasites probed with *rif3* antiserum. Lanes: 1, uninfected red cells; 2, PAR^+; 3, PAR^-; 4, T9/96; 5, R29; 6, A4; 7, C10; 8, C18; 9, 3D7. The 30-kDa and 46-kDa molecular mass markers are shown. (*b*) Immunoprecipitation of ^{35}S metabolically labeled extracts from PAR^+. Lanes: 1, rabbit preimmune serum; 2, *rif1* antiserum. (*c*) Immunoprecipitation of extracts from ^{125}I-surface-labeled PAR^+-infected red cells. Lanes: 1 and 2, mock-trypsinized; 3 and 4, treated with trypsin at 1 mg/ml, followed by trypsin inhibitor; 1 and 3, preimmune serum; 2 and 4, *rif1* antiserum. (*d* and *e*) Immunoprecipitation of triton-insoluble extracts from ^{35}S metabolically labeled A4-infected red cells. Lanes: 1, mock-trypsinized; 2, treated with trypsin at 1 mg/ml, followed by trypsin inhibitor. (*d*) *rif3* antiserum. (*e*) MESA antiserum.

To determine the cellular localization of the rifins, we first carried out an indirect immunofluorescence assay (IFA) with the *rif1* and *rif3* antisera to probe fixed thin films of PAR^+-infected red cells. Both cytosolic and red cell membrane-associated fluorescence were evident in the majority (>95%) of mature trophozoite-infected cells (Fig. 4). Occasional mature parasitized cells were 4,6-diamidino-2-phenylindole-positive but immunofluorescence-negative (Fig. 4*b*, *Lower left*). Ring stage parasites showed faint fluorescence over the parasite itself, but no red cell cytoplasm or red cell membrane fluorescence (data not shown).

It was not possible to determine from the IFA results whether or not rifins are exposed on the extracellular surface of infected cells. We therefore carried out immunoprecipitation with the *rif* antisera of extracts from intact infected red cells of PAR^+ that had been surface-labeled with ^{125}I. Specific bands of the expected size were precipitated (Fig. 3*c*, lanes 1 and 2), but these bands were not seen when the infected cells were trypsinized after labeling, confirming the exposure of rifins on the infected red cell surface (Fig. 3*c*, lanes 3 and 4). A trypsin-sensitive 39-kDa band was also immunoprecipitated from surface-labeled extracts of the A4 clone, but no bands were seen with T9/96 (data not shown). To exclude the possibility that the relatively high concentration of trypsin used compromised the integrity of the membrane and thus cleaved internal proteins, we carried out a metabolic labeling of A4 infected cells, followed by trypsinization and immunoprecipitation with anti-rifin antibodies and antibodies to two internal parasite proteins associated with the infected red cell membrane [MESA (33) and HRP1(34)]. A 39-kDa rifin band was

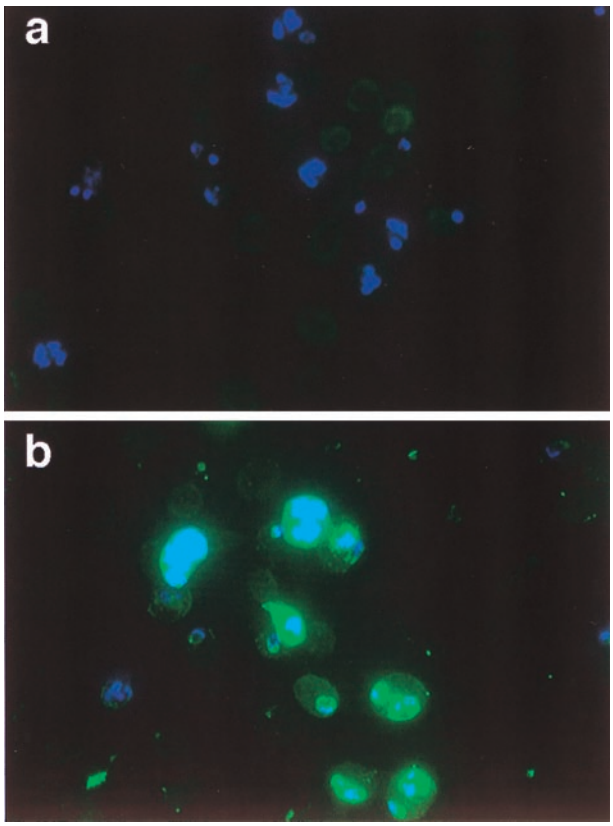

FIG. 4. IFA of fixed PAR^+-infected red cells. (*a*) Preimmune serum. (*b*) *Rif3* antiserum. The secondary antibody was FITC-conjugated swine anti-rabbit immunoglobulins (green), and parasite nuclei were stained with 4,6-diamidino-2-phenylindole (blue). The *rif1* antiserum gave similar results.

precipitated from intact A4 cell extracts but not from extracts of trypsin-treated cells (Fig. 3*d*), whereas a MESA band (Fig. 3*e*) and HRP1 proteins (data not shown) are immunoprecipitated at equal intensity from both extracts.

Despite their presence on the cell surface, pooled adult immune sera from Kenya or the Gambia failed to immunoprecipitate surface-labeled proteins with the characteristics of rifins from either PAR^+ or A4 parasites (data not shown). Whether this means that the sequences are too diverse to be detected with anything other than homologous antibody, that they are not naturally immunogenic, or that the immune response is very short-lived remains to be determined.

We also attempted to use the *rif1* and *rif3* antisera to detect rifins on unfixed infected cells by flow cytometry analysis and by IFA and microscopy. Neither of the antisera reacted with unfixed PAR^+ or PAR^- parasites, suggesting that the GST fusion proteins are not conformationally correct and only elicit antibodies to linear determinants not accessible at the infected red cell surface. Alternatively, it is possible that the antisera recognize mainly the semiconserved N-terminal region of the protein that is predicted to be intracellular, rather than the extracellular, variable region.

Rifins Are Clonally Variant. To analyze further how the rifins are expressed in other parasite genotypes, we repeated the Western blots on the isolates tested above for transcription. The antisera detected proteins in the range of 35–44 kDa in a number of these parasites (Fig. 3*a*). Clones A4, C10, and C18, which are genetically identical but differ in adhesion phenotype and surface antigenicity (12), showed different combinations of rifin proteins (Fig. 3*a,* lanes 6, 7, and 8), indicating clonal variation in expression and suggesting a possible link between rifins and parasite adhesion. Consistent with the Northern blot data, rifins were not detected by Western blotting in the parasite clone R29 (Fig. 3*a*, lane 5). In parasites T9/96 and 3D7, however, the 44-kDa rifin was detected (Fig. 3*a*, lanes 4 and 9), despite the absence of detectable *rif* RNA on the Northern blot (Fig. 2*b*, lanes 3 and 8). Noting also that protein detected in PAR^- is low relative to PAR^+, this suggests that the *rif* antisera and the complex *rif* probe used in the hybridizations do not entirely overlap in specificity. The antisera also recognized proteins of 50 kDa and around 70 kDa in Western blots of all the parasites studied (data not shown). These latter proteins may either represent antigenically cross-reactive proteins or products of some as yet unidentified abnormal splicing event.

Rifins Are Semiresistant to Trypsin Treatment, in Parallel with the Partial Trypsin Resistance of Rosetting in Some Parasites. Proteins with the characteristics of rifins (strain-specific surface-labeled low molecular weight proteins) had originally been named rosettins and were purported to mediate rosetting (22). However, recent data clearly indicate that PfEMP1 is a major rosetting ligand (8, 9). It remains possible that rifins may act as accessory molecules in rosetting or may be necessary for rosetting in isolates that do not express a rosetting-type PfEMP1 variant. One of the characteristics of PfEMP1 is its exquisite sensitivity to proteases, being cleaved by as little trypsin as 1 μg/ml (16, 29). We therefore compared the trypsin sensitivity of rosetting and rifins in PAR^+, to determine whether rifins might play a role in rosetting in this clone. With trypsin at both 10 μg/ml and 100 μg/ml, PfEMP1 is removed (16, 29) but rifins are almost untouched (Fig. 5 *a* and *b*), and rosetting is mostly, but not completely, disrupted (Fig. 5*c*). With trypsin at 1 mg/ml, when both rifins and PfEMP1 have been removed, rosetting is abolished. Thus, there is a small component of rosetting in PAR^+ that is relatively trypsin-resistant and could be rifin-mediated. In contrast, in the R29 clone, in which *rif* RNA and rifin protein cannot be detected (Figs. 2*b* and 3*a*), rosetting is completely abolished by trypsin 10 μg/ml (data not shown), which is consistent with a purely PfEMP1-mediated rosetting mechanism in this parasite.

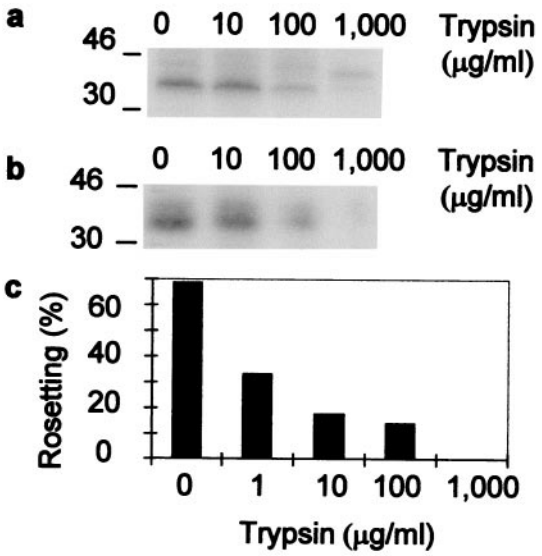

FIG. 5. Trypsin sensitivity of rifins and rosetting in PAR^+. PAR^+-infected red cells were surface-labeled with ^{125}I and then treated with various concentrations of trypsin. (*a*) Total Triton X-100-soluble extracts. (*b*) Triton X-100-soluble extracts immunoprecipitated with *rif3* antiserum. Both were subjected to SDS/PAGE. (*c*) Rosetting of trypsinized infected cells. The percentage rosetting indicates the proportion of mature infected red cells binding two or more uninfected red cells. The data are from a representative experiment, and three further repetitions gave similar results.

Attempts to show direct binding of the purified recombinant *rif1* and *rif3* proteins to uninfected red cells were unsuccessful, despite using a variety of methods. However, because we had already shown that antisera raised to these fusion proteins did not bind to intact infected cells, it is likely that even if the rifins are capable of interacting with erythrocytes, we would not have detected it with these constructs.

DISCUSSION

We have confirmed that members of the *rif* gene family are transcribed in asexual stage parasites. We have also shown that they are translated into rifin proteins that are expressed on the surface of infected red cells and are phenotypically variable. Whereas our data are consistent with rifins playing an accessory role in rosette formation in some parasite isolates, we do not believe that this is their primary function, because many parasites that do not show appreciable levels of rosetting still express them. Whether this function is related to parasite adhesion or some other aspect of parasite biology within the vertebrate host awaits further experimentation.

The genomic location of *rif* and *var* sequences suggests that telomeres play an important role in antigenic variation. Thus, we determined the relative timing of transcription of both variant multigene families and found that abundant *rif* transcripts of the expected 1.8- to 2.1-kb range occur for only a short time at the transition between rings and pigmented trophozoites, whereas *var* gene expression starts in early ring stages and continues until late rings. It has been suggested that *var* gene transcription could be controlled through modifications in chromatin structure (35). Our data do not support or refute this model but do imply that control of *var* gene expression is not simply the opening of a telomeric site for general transcription. The ORFs nearby may be involved in this control, but we still have no evidence for how this may happen.

Although initial reports suggested that *rif* genes are transcribed at schizont stages, the timing discrepancy can be explained by the methods used in the previous reports. One report used dot blots of staged RNA (17), and the other used RT-PCR (19). Dot blots would not discern between RNA and small amounts of contaminating DNA, which we have noticed hybridizes extremely efficiently with *rif* probes because of the high copy number in the genome. Our earliest attempts at extracting RNA from schizonts were complicated by the additional genomic DNA relative to RNA, and improvements on the extraction procedure were necessary to separate the two nucleic acids. RT-PCR is highly sensitive, and although a low level of message can be detected in multinucleate schizonts, the stage for maximal expression of the 1.8- to 2.1-kb transcript is earlier, before nuclear division.

We have attempted to confirm clonal variation in expression of these proteins by analyzing transcripts from a clone tree by RT-PCR. To date, these data have been inconclusive, because the high degree of diversity between *rif* sequences makes universal primer design difficult, and we have seen highly significant bias in the sequences amplified by a range of primers that we have tried. Although sequencing of transcripts would be the gold standard for clonal variation, we believe that the Western blot data are convincing evidence in itself. It would clearly be of interest also to know whether expressed *rif* sequences are derived from the same telomere (or internal genomic location) as the expressed *var* gene in a given parasite clone. The difficulty in designing universal primers, however, means that we have not yet been able to amplify efficiently the major *rif* transcripts, so this question requires further experimentation.

The surface of the infected erythrocyte is the major interface between the host and the parasite during asexual blood infection by *P. falciparum*. It is already known that PfEMP1 molecules, which are expressed at this site in a clonally variable manner, are implicated in both the pathogenesis of severe disease and the induction of protective immunity. The fact that a second clonally variable set of proteins, the rifins, are expressed at the infected red cell surface suggests that an important evolutionary advantage is conferred by their presence. It will be crucial therefore to elucidate the function of these proteins before further progress can be made in understanding the processes that underlie pathogenesis, immunity, and parasite survival in the human host.

We thank Daniel Lawson and Bart Barrell from The Sanger Centre for their help with genome analysis; Margaret Jones, Department of Cellular Science, Oxford, for help with IFA images; Bob Pinches, Molecular Parasitology Group, Oxford, for parasite culture; and Jeff Lyon for the anti-MesA antibody. Sequencing of chromosomes 2 and 3 was part of the International Malaria Genome Sequencing Project and was supported by The Wellcome Trust, the National Institute of Allergy and Infectious Diseases, and the U.S. Department of Defense. This work was funded by The Wellcome Trust.

1. Newbold, C. I., Craig, A. G., Kyes, S., Berendt, A. R., Snow, R. W., Peshu, N. & Marsh, K. (1997) *Ann. Trop. Med. Parasitol.* **91,** 551–557.
2. Kaul, D. K., Roth, E. F., Jr., Nagel, R. L., Howard, R. J. & Handunnetti, S. M. (1991) *Blood* **78,** 812–819.
3. Warrell, D. A. (1987) *Parasitology* **94,** S53–S76.
4. Aley, S. B., Sherwood, J. A. & Howard, R. J. (1984) *J. Exp. Med.* **160,** 1585–1590.
5. Magowan, C., Wollish, W., Anderson, L. & Leech, J. (1988) *J. Exp. Med.* **168,** 1307–1320.
6. Baruch, D. I., Gormely, J. A., Ma, C., Howard, R. J. & Pasloske, B. L. (1996) *Proc. Natl. Acad. Sci. USA* **93,** 3497–3502.
7. Baruch, D. I., Ma, X. C., Singh, H. B., Bi, X., Pasloske, B. L. & Howard, R. J. (1997) *Blood* **90,** 3766–3775.
8. Rowe, J. A., Moulds, J. M., Newbold, C. I. & Miller, L. H. (1997) *Nature (London)* **388,** 292–295.
9. Chen, Q., Barragan, A., Fernandez, V., Sundstrom, A., Schlichtherle, M., Sahlen, A., Carlson, J., Datta, S. & Wahlgren, M. (1998) *J. Exp. Med.* **187,** 15–23.
10. Gardner, J. P., Pinches, R. A., Roberts, D. J. & Newbold, C. I. (1996) *Proc. Natl. Acad. Sci. USA* **93,** 3503–3508.
11. Bull, P. C., Lowe, B. S., Kortok, M., Molyneux, C. S., Newbold, C. I. & Marsh, K. (1998) *Nat. Med.* **4,** 358–360.
12. Roberts, D. J., Craig, A. G., Berendt, A. R., Pinches, R., Nash, G., Marsh, K. & Newbold, C. I. (1992) *Nature (London)* **357,** 689–692.
13. Smith, J. D., Chitnis, C. E., Craig, A. G., Roberts, D. J., Hudson-Taylor, D. E., Peterson, D. S., Pinches, R. A., Newbold, C. I. & Miller, L. H. (1995) *Cell* **82,** 101–110.
14. Su, X.-Z., Heatwole, V., Wertheimer, S., Guinet, F., Herrfeldt, J. A., Peterson, D. S., Ravetch, J. A. & Wellems, T. E. (1995) *Cell* **82,** 89–100.
15. Baruch, D. I., Pasloske, B. L., Singh, H. B., Bi, X., Ma, X. C., Feldman, M., Taraschi, T. F. & Howard, R. J. (1995) *Cell* **82,** 77–87.
16. Leech, J. H., Barnwell, J. W., Miller, L. H. & Howard, R. J. (1984) *J. Exp. Med.* **159,** 1567–1575.
17. Weber, J. L. (1988) *Mol. Biochem. Parasitol.* **29,** 117–124.
18. Gardner, M. J., Tettelin, H., Carucci, D. J., Cummings, L. M., Aravind, L., Koonin, E. V., Shallom, S., Mason, T., Yu, K., Fujii, C., *et al.* (1998) *Science* **282,** 1126–1132.
19. Cheng, Q., Cloonan, N., Fischer, K., Thompson, J., Waine, G., Lanzer, M. & Saul, A. (1998) *Mol. Biochem. Parasitol.* **97,** 161–176.
20. Carcy, B., Bonnefoy, S., Guillotte, M., Le Scanf, C., Grellier, P., Schrevel, J., Fandeur, T. & Mercereau-Puijalon, O. (1994) *Mol. Biochem. Parasitol.* **68,** 221–233.
21. Limpaiboon, T., Taylor, D. W., Jones, G., Geysen, H. M. & Saul, A. (1990) *Southeast Asian J. Trop. Med. Public Health* **21,** 388–396.
22. Helmby, H., Cavelier, L., Pettersson, U. & Wahlgren, M. (1993) *Infect. Immun.* **61,** 284–288.
23. Genetics Computer Group (1994) Program Manual for the Wisconsin Package, Version 8. (Genetics Computer Group, Madison, WI).
24. Hofmann, K. & Stoffel, W. (1993) *Biol. Chem. Hoppe-Seyler* **347,** 166.
25. Persson, B. & Argos, P. (1994) *J. Mol. Biol.* **237,** 182–192.
26. Persson, B. & Argos, P. (1996) *Protein Sci.* **5,** 363–371.
27. Nielsen, H., Engelbrecht, J., Brunak, S. & von Heijne, G. (1997) *Protein Eng.* **10,** 1–6.
28. Lambros, C. & Vanderberg, J. P. (1979) *J. Parasitol.* **65,** 418–420.
29. Fernandez, V., Treutiger, C. J., Nash, G. B. & Wahlgren, M. (1998) *Infect. Immun.* **66,** 2969–2975.
30. Goda, S. K. & Minton, N. P. (1995) *Nucleic Acids Res.* **23,** 3357–3358.
31. Rubio, J. P., Thompson, J. K. & Cowman, A. F. (1996) *EMBO J.* **15,** 4069–4077.
32. Harlow, E. & Lane, D. (1988) in *Antibodies: A Laboratory Manual* (Cold Spring Harbor Lab. Press, Plainview, NY), pp. 53–138.
33. Coppel, R. L., Lustigman, S., Murray, L. & Anders, R. F. (1988) *Mol. Biochem. Parasitol.* **31,** 223–231.
34. Pasloske, B. L., Baruch, D. I., van Schravendijk, M. R., Handunnetti, S. M., Aikawa, M., Fujioka, H., Taraschi, T. F., Gormley, J. A. & Howard, R. J. (1993) *Mol. Biochem. Parasitol.* **59,** 59–72.
35. Scherf, A., Hernandez-Rivas, R., Buffet, P., Bottius, E., Benatar, C., Pouvelle, B., Gysin, J. & Lanzer, M. (1998) *EMBO J.* **17,** 5418–5426.